Copper complex of polyglycerol anchored onto graphene oxide as a recyclable nanocatalyst for sonochemical green synthesis of naphthoquinones

Hossein Naeimi* and Maryam Farahnak Zarabi

Department of Organic Chemistry, Faculty of Chemistry, University of Kashan, Kashan, 87317, I. R. Iran; Fax: +98-03155912397; Tel: +98-03155912388;

E-mail: naeimi@kashanu.ac.ir.

Abstract:

In the present study, Cu (II) immobilized on hyperbranched polyglycerol functionalized graphene oxide catalyst was prepared as a novel, green, highly efficient and reusable heterogeneous catalyst. Then, the synthesis of naphthoquinone derivatives was performed by the employment of Go-HPG-IA-Cu(II) as catalyst under ultrasound irradiation to afford the desired products in high yields and short reaction times. Also, this catalyst could be easily recovered and reused several times without any significant loss of its catalytic activity.

Keywords: Graphene oxide, Hyperbranched polyglycerol, Catalyst, Naphthoquinone, Ultrasound,

Introduction

Fluorescent materials are of interest in many disciplines such as emitters for electroluminescence devices [1], molecular probes for biochemical research [2], in traditional textile and polymer fields [1], fluorescent whitening agents [3] and photo conducting materials [4]. Molecules with the napthoquinone structure were reported as fluorescence compounds [5]. Also, these molecules are interested because of widespread biological properties, their industrial applications, and their potential as intermediates in the synthesis of heterocycles[5]. Because of their common applications, several methods have been reported for synthesis of these compounds. Hydroxyl naphthalene-1,4-dione derivatives have been synthesized in the presence of different catalystssuch asdodecyl benzenesulfonic acid [6],Ionic liquids [7], MCM-41 [5], *p*-TsOH[8], $ZrOCl_2$[9], $InCl_3$[4], and nano copper(II) oxide[10].

Graphene, a monolayer of carbon atoms packed into a dense honeycomb crystal structure, has attached much attention due to its unique properties such as a large theoretical specific surface area (2630 m^2g^{-1}), high intrinsic mobility (200 000 $cm^2\ v^{-1}\ s^{-1}$) [11-12], high Young's modulus (~1.0 TPa)[13] and thermal conductivity (~5000 $Wm^{-1}K^{-1}$) [14], and its optical transmittance (~97.7%) and good electrical conductivity [15-16]. Graphene oxide (GO), oxidized form of graphene, is usually produced by the chemical oxidation of graphite, with subsequent dispersion and exfoliation in water or suitable organic solvents [17].

The structure of graphene oxide have been identified with oxygen functionalities such as hydroxyl and epoxy groups on the basal plane, and with smaller amounts of carboxy, carbonyl, phenol, lactone, and quinone at the sheet edges [18-20]. The presence of these functional groups can also provide sites for chemical modification or functionalization of GO through covalent or noncovalent bonds for numerous applications [21]. The study of GO-based catalysts in recent years has been popular and extensive.

Hyperbranched polymers are highly branched macromolecules with three-dimensional dendritic architecture. Due to their unique chemical and physical properties and potential applications in various fields is growing rapidly [22]. A class of hyperbranched polymers are the aliphatic polyether polyols named polyglycerol[23-24]. Glycidol is the basic monomer to produce polyglycerol. It is a commercially available and highly reactive hydroxy epoxide, can be polymerized to polyglycerol using nucleophilic initiators such as alkoxides[25-27]. The distinctive characteristic of hyperbranched polyglycerol is their highly branched structure containing many hydroxyl groups on the surface, which can increase the functionalizing with different functional groups covalently or non-covalently to obtain novel nanostructures [28].

Based on the green chemistry principles, synthetic methods should be use materials that display little or no toxicity to the environment and human health [29]. Therefore, Cu (II) salt has attracted attention owing to their ease of handling, low toxicity, low cost and relative insensitivity to air and moisture.

Ultrasound irradiation has progressively been considered as a convenient and clean synthetic approach [30]. Ultrasonic irradiation leads to acoustic cavitation, which collapse of bubbles generates localized hot spots with very short lifetimes and extremely high pressures and temperatures [31]. Ultrasonic activation is increased reaction rates, formation of pure products in high yields, easier manipulation, and mild reaction conditions [32-34] which compared with traditional methods, this technique is more suitable taking green chemistry concepts into account [30, 35].

Herein, we would like to describe a highly efficient method for the preparation of naphthoquinone derivatives via the one-pot three-component condensation reactionin the presence of Cu (II) immobilized on hyperbranched polyglycerol functionalized graphene oxide as an efficient and reusable heterogeneous catalyst under ultrasound irradiation.

Experimental

The chemicals were purchased from Fluka and Merck Chemical Companies and used without purification. IR spectra were obtained as KBr pellets on a Perkin-Elmer 781 spectrophotometer and on an impact 400 Nicolet FT-IR spectrophotometer. ^{1}H NMR was recordedin DMSO-d_6 solvent on a Bruker DRX-400 spectrometer with tetramethylsilane as internal reference.XRD patterns were obtained by an X'PertPro (Philips) instrument with 1.54 °A wavelengths of X-ray beam and Cu anode material, at a scanning speed of 2° min^{-1} from 10° to 80° (2Ɵ). Thermogravimetric analysis (TGA) was performed on a mettler TA4000 system TG-50 at a heating rate of 10 K min^{-1} under N_2 atmosphere. The SEM images of catalysts were recorded on a FE-SEM Hitachi S4160 instrument. The AFM image of catalystswas investigated using scanning probe microscopy (SPM-9600, Shimadzu). Also, elemental analyses for catalyst with inductively coupled plasma atomic emission spectroscopy were obtained from an ICP-OES simultaneous instrument VISTA-PRO Model. A Bandelin ultrasonic HD 3200 with 6 mm diameter model KE 76 probe was used to generate ultrasonic irradiation and homogenize the reaction mixture. The piezoelectric crystals in this kind of probe normally work at approximately 700 kHz; by use of appropriate clamps. However, the output frequency of piezoelectric crystals was controlled and reduced to 20 kHz in the reaction mixture. Melting points were measured with a Yanagimoto micro melting point apparatus. The purity determination of the substrates and reaction monitoring were accomplished by TLC on silica-gel polygram SILG/UV 254 plates (from Merck Company).

Preparation of catalyst

Preparation of graphene oxide

The graphene oxide nanosheets were synthesized by a modified Hummer's method. Typically, in a 1000 mL round-bottom flask equipped with a magnetic bar, a mixture of 5.0 g of natural graphite powder and 2.5 g of sodium nitrate and 115 mL of sulfuric acid (98%) were placed in an ice bath. Then, 15.0 g of potassium permanganate was slowly added to obtained solution and stirred for 2 h. The mixture solution was taken to a water bath (35 °C) and stirred for 30 min. Then, deionized water (230 mL) was slowly added and the solution temperature was about 98 °C and stirred for 15 min. Afterward, 700 mL of deionized water and 50 mL of H_2O_2 (30%) was added to the solution respectively. The resulting materials were filtered and washed by diluted HCl (5%) and deionized water for several times. Then graphite oxide powder was obtained after drying for 12 h at 60 °C under vacuum. The graphite oxide powder was dispersed in distilled water to make concentration of 0.5 mg mL^{-1} and exfoliated by ultrasonication to obtain GO nanosheets.

Grafting of hyperbranchedpolyglycerol on GO nanosheets

The hyperbranched polyglycerol modified GO nanosheets were prepared according to the reported protocol with minor revision [36]. A saturated solution of potassium methoxide in methanol was mixed with 0.2 g of graphene oxide nanosheets. The mixture was sonicated in an ultrasonic bath for 30 min and stirred at room temperature for 2 h. Then, mixture was refluxed at 80 °C for 4 h. After completion of the reaction, graphene oxide nanosheets were washed with methanol and dried in a vacuum oven at 60 °C. The glycidol (4 mL) was added slowly to deprotonated nanosheets at 100 °C and the mixture was stirred at 100 °C for 8 h. Then it was cooled and the mixture was dissolved in methanol. After repeated wash by methanol followed by drying overnight under vacuum, HPG grafted on graphene oxide nanosheets (GO-HPG) was obtained. The synthesis of hyperbranched polyglycerol functionalized graphene oxide was confirmed by IR and TGA.

Preparation of GO-HPG-IA

In a round-bottomed flask, GO-HPG (0.2 g) and isatoic anhydride (0.2 g) was suspended in 30 mL ethanol and subsequently, the reaction mixture was refluxed at 60 °C for 24 h. Subsequently formed mixture was washed several times with ethanol and dried under vacuum at 70°C for 24 h.

Preparation of GO-HPG-IA- Cu (II)

In the final of catalyst preparation, GO-HPG-IA (0.2 g) and copper (II) acetate (0.2 g) was suspended in 20 mL acetonitrile. Then, the reaction mixture was refluxed at 60 °C for 24 h. The reaction mixture was filtered and washed with acetonitrile to ensure that the excess copper (II) acetate was completely removed. Finally, the products were dried at 70 °C under vacuum, the pure complex was obtained.

General procedure for the preparation of aminonaphthoquinonederivatives catalyzed by GO-HPG-IA- Cu (II) under ultrasound irradiation

A mixture of 2-hydroxy-1,4-naphthoquinone (1 mmol), aldehyde (1 mmol), amine (1 mmol), catalyst GO-HPG-IA- Cu (II) (15 mg, 0.1 mol% Cu) in EtOH (2mL) was sonicated at 40 kHz at room temperature for the appropriate time according to Table **2**. The progress of the reaction was monitored by thin layer chromatography (TLC) and was used n-hexane/ethyl acetate as an eluent. After completion of the reaction, the mixture was diluted with dichloromethane and the catalyst was filtered and washed with chloroform and EtOH for checking the reusability. The solution was recovered via evaporation using a rotary evaporator. The organic residue was washed with cold ethanol for several times and dried under vacuum to give the pure product. The products were confirmed by spectral data and physical data.

2-((4-Chlorophenyl)((4-methoxyphenyl)amino)methyl)-3-hydroxynaphthalene-1,4-dione (4a)

Yellow solid, mp. 125-127 °C (lit. [37]: 127-128 °C); IR (KBr, ν, cm^{-1}): 3428, 3070, 1685, 1616, 1539, 1487, 1224, 1173 ;^{1}H NMR (400 MHz, DMSO-d_6) (δ, ppm): 3.63 (s, 3H), 6.58 (s, 1H), 7.29-7.31 (m, 4H), 7.49-7.50 (m, NH), 7.58-7.59 (m, 4H), 7.83-7.88 (m, 2H), 7.98-8.0(m, 1H), 8.05-8.09 (m, 1H), 8.82 (s, OH).

2-((4-Bromophenyl)((4-methoxyphenyl)amino)methyl)-3-hydroxynaphthalene-1,4-dione (4b)

Brown solid, mp. 135-136 °C; IR (KBr, ν, cm^{-1}): 3437, 3072, 1678, 1614, 1535, 1488, 1261, 1175; ^{1}H NMR (400 MHz, DMSO-d_6) (δ, ppm): 3.64 (s, 3H), 6.58 (s, 1H), 7.25 (d, ^3J =8.0 Hz, 2H),7.43 (s, NH), 7.55-7.64 (m, 4H), 7.74 (d, ^3J =8.0 Hz, 2H), 7.85-7.88(m, 2H), 7.99 (d, ^3J =8.0 Hz, 1H), 8.09 (d, ^3J =8.0 Hz, 1H), 8.81(s, OH).

2-((4-Fluorophenyl)((4-methoxyphenyl)amino)methyl)-3-hydroxynaphthalene-1,4-dione (4c)

Brown solid, mp. 160-165 °C; IR (KBr, ν, cm^{-1}): 3424, 3054, 1684, 1611, 1541, 1496, 1271, 1223, 1170; ^{1}H NMR (400 MHz, DMSO-d_6) (δ, ppm): 3.63 (s, 3H), 6.59 (s, 1H), 7.04-7.07 (s, NH),7.33-7.35 (m, 4H), 7.54-7.56 (m, 2H), 7.61-7.62 (m, 2H), 7.85-7.86 (m, 2H), 7.98-8.0 (m, 1H), 8.03-8.08 (m, 1H), 8.81(s, OH).

2-Hydroxy-3-(((4-methoxyphenyl)amino)(p-tolyl)methyl)naphthalene-1,4-dione (4d)

Brown solid, mp. 170-174°C; IR (KBr, ν, cm^{-1}): 3432, 2923, 1678, 1615, 1540, 1497, 1270, 1170; ^{1}H NMR (400 MHz, DMSO-d_6) (δ, ppm): 2.47 (s, 3H), 3.63 (s, 3H), 6.68 (s, 1H), 7.16-7.17 (m, 2H), 7.32-7.34 (m, 2H), 7.55-7.64 (m, 4H), 7.85-7.88(m, 2H), 7.99-8.0 (m, 1H), 8.08-8.10 (m, 1H), 8.83(s, OH).

2-((4-Chlorophenyl)((4-nitrophenyl)amino)methyl)-3-hydroxynaphthalene-1,4-dione (4e)

Orange solid, mp. 128-130 °C (lit.[37]: 132-133 °C); IR (KBr, ν, cm^{-1}): 3200, 3031, 1678, 1605, 1570, 1518, 1492, 1356; ^{1}H NMR (400 MHz, DMSO-d_6) (δ, ppm): 6.12(s, 1H), 7.40-7.42 (m, 4H),7.47-7.49 (m, 4H), 7.76-7.80 (m, 1H), 7.83-7.87 (m, 1H), 7.94 (d, ^3J =8.0 Hz, 1H), 8.05 (d, ^3J =8.0 Hz, 1H), 9.29 (s, OH).

2-((4-Bromophenyl)((4-nitrophenyl)amino)methyl)-3-hydroxynaphthalene-1,4-dione (4f)

Orange solid, mp. 128-130 °C; IR (KBr, ν, cm^{-1}): 3191, 3062, 1667, 1593, 1574, 1504, 1347; ^{1}H NMR (400 MHz, DMSO-d_6) (δ, ppm): 6.11(s, 1H), 7.40-7.42 (m, 4H),7.47-7.49 (m, 4H), 7.78 (t, ^3J =8.0 Hz, 1H), 7.85 (t, ^3J =8.0 Hz, 1H), 7.94 (d, ^3J =8.0 Hz, 1H), 8.05 (d, ^3J =8.0 Hz, 1H), 9.29 (s, OH).

2-Hydroxy-3-((4-nitrophenyl)((4-nitrophenyl)amino)methyl)naphthalene-1,4-dione (4g)

Yellow solid, mp. 134-137 °C (lit. [37]: 135-136 °C); IR (KBr, ν, cm^{-1}): 3197, 3076, 1668, 1609, 1591, 1516, 1346; ^{1}H NMR (400 MHz, DMSO-d_6) (δ, ppm): 6.11(s, 1H), 7.40-7.42 (m, 4H),7.47-7.49 (m, 4H), 7.78 (t, ^3J =8.0 Hz, 1H), 7.85 (t, ^3J =8.0 Hz, 1H), 7.94 (d, ^3J =8.0 Hz, 1H), 8.05 (d, ^3J =8.0 Hz, 1H), 9.28 (s, OH).

2-Hydroxy-3-(((4-nitrophenyl)amino)(p-tolyl)methyl)naphthalene-1,4-dione (4h)

Orange solid, mp. 146-148 °C (lit. [37]: 145-147 °C); IR (KBr, ν, cm^{-1}): 3198, 3074, 1667, 1610, 1591, 1506, 1349; ^{1}H NMR (400 MHz, DMSO-d_6) (δ, ppm): 2.33 (s, 3H), 6.11(s, 1H), 7.40-7.42 (m, 4H),7.47-7.49 (m, 4H), 7.77-7.80 (m, 1H), 7.83-7.87 (m, 1H), 7.93-7.94 (m, 1H), 8.04-8.06 (m, 1H), 9.28 (s, OH).

2-((4-Chlorophenyl)(m-tolylamino)methyl)-3-hydroxynaphthalene-1,4-dione (4i)

Brown solid, mp. 150-153 °C; IR (KBr, ν, cm^{-1}): 3414, 3070, 1680, 1596, 1540, 1487; ^1H NMR (400 MHz, DMSO-d_6) (δ, ppm): 2.39 (s, 3H), 6.34 (s, 1H), 6.81-6.83 (m, 1H), 7.14-7.16 (m, 1H), 7.30-7.32 (m, 2H), 7.47 (s, NH), 7.61-7.70 (m, 4H), 7.77-7.79 (m, 1H), 7.90-7.94 (m, 1H), 8.04-8.05 (m, 1H),8.10-8.12 (m, 1H), 8.91(s, OH).

2-((4-Bromophenyl)(m-tolylamino)methyl)-3-hydroxynaphthalene-1,4-dione (4j)

Yellow solid, mp. 147-150 °C; IR (KBr, ν, cm^{-1}): 3403, 3068, 1680, 1595, 1539, 1485; ^1H NMR (400 MHz, DMSO-d_6) (δ, ppm): 2.37 (s, 3H), 6.34 (s, 1H), 6.82-6.83 (m, 1H), 7.12-7.13 (m, 1H), 7.23-7.27 (m, 2H), 7.67-7.69(m, 1H), 7.75-7.77 (m, 4H), 7.90-7.93 (m, 1H), 8.02-8.04 (m, 1H), 8.08-8.10 (m, 1H), 8.90(s, OH).

2-((4-Fluorophenyl)(m-tolylamino)methyl)-3-hydroxynaphthalene-1,4-dione (4k)

Yellow solid, mp. 143-146 °C; IR (KBr, ν, cm^{-1}): 3382, 3061, 1685, 1600, 1541, 1509, 1220; ^1H NMR (400 MHz, DMSO-d_6) (δ, ppm): 2.38 (s, 3H), 6.34 (s, 1H), 6.81-6.83 (m, 1H), 7.14 (m, 2H), 7.33-7.39 (m, 4H), 7.67-7.69 (m, 1H), 7.75-7.77 (m, 1H), 7.89-7.91 (m, 1H), 8.03-8.05 (m, 1H),8.08-8.10 (m, 1H), 8.89(s, OH).

2-Hydroxy-3-((4-methoxyphenyl)(m-tolylamino)methyl)naphthalene-1,4-dione (4l)

Brown solid, mp. 144-147°C; IR (KBr, ν, cm^{-1}): 3327, 3010, 1683, 1607, 1538, 1509, 1246, 1175; ^1H NMR (400 MHz, DMSO-d_6) (δ, ppm): 2.37 (s, 3H), 3.87 (s, 3H), 6.34 (s, 1H), 6.73-6.77 (m, 1H), 6.80-6.83 (m, 1H), 7.10-7.14 (m, 2H), 7.20-7.23 (m, 4H), 7.67-7.68 (m, 1H), 7.75-7.76 (m, 1H), 7.90-7.93 (m, 1H), 8.01-8.09 (m, 1H), 8.90(s, OH).

2-Hydroxy-3-(m-tolyl(p-tolylamino)methyl)naphthalene-1,4-dione (4m)

Brown solid, mp. 146-149 °C; IR (KBr, ν, cm^{-1}): 3326, 3027, 1669, 1602, 1526, 1298; ^1H NMR (400 MHz, DMSO-d_6, - $CDCl_3$) (δ, ppm): 2.31 (s, 3H), 2.37 (s, 3H), 6.03 (s, 1H), 7.16

(d, ^3J =8.0 Hz, 2H), 7.35 (d, ^3J =8.0 Hz, 2H), 7.67 (t, ^3J =8.0 Hz, 1H), 7.77 (t, ^3J =8.0 Hz, 1H), 7.83-7.86 (m, 1H), 7.92-7.94 (m, 2H), 8.02-8.06 (m, 2H),8.08-8.10 (d, ^3J =8.0 Hz, 1H), 8.91 (s, OH).

Results and Discussion

The process for the preparation of GO-HPG-IA-Cu (II) catalyst is described in Scheme **1**. First, graphene oxide nanosheets were prepared using a modified Hummer's method. There was a great amount of active hydrogen-containing functional groups including hydroxyl and carboxylic acid groups on graphene oxide nanosheets surface. Hyperbranched polymerization of glycidol was initiated by these active surface groups on graphene oxide nanosheets, producing a high hydrophilic PG layer on graphene oxide surface [38]. The obtained hyperbranched polyglycerol functionalized graphene oxide was then treated with isatoic anhydride to generate GO-HPG-IA. Finally, the GO-HPG-IA-Cu (II) was easily prepared by reaction of GO-HPG-IA with $Cu(OAc)_2$. After successful preparation of the GO-HPG-IA-Cu (II), the catalyst was characterized by FT-IR, TGA, XRD, AFM, and FESEM.

Scheme 1. Preparation of GO-HPG-IA-Cu(II) nanocatalyst.

Figure **1a–d** shows the FT-IR spectra of graphite, GO, GO-HPG, and GO-HPG-IA, respectively. The FT-IR spectrum of graphite powder shows peaks characteristic of C=C groups at 1573 cm^{-1} which the peak is not sharp (Figure **1a**). Figure **1b** shows the FT-IR spectrum of graphene oxide powder. The absorption band at 1578 cm^{-1} is related to C=C double bonds which this peak is sharper than graphite due to the unsymmetry of GO. The absorption peaks at 1030, 1720 and 3410 $cm^{-1}$are assigned to C–O, carbonyl, and hydroxyl

stretching mode of functional groups attachment to GO, respectively. Figure **1c** shows the FT-IR spectrum of the GO-HPG. The vibrational bands at 2922 cm^{-1} and 2853 cm^{-1} are attributed to C-H stretching, which confirmed that the HPG had been successfully grafted on the surface of graphene oxide. In the FT-IR spectrum of the GO-HPG-IA, the peak at 1741 cm^{-1} is attributed to ester bonds which indicates that the terminal hydroxyl groups is replaced by isatoic anhydride and the GO-HPG-IA had been successfully obtained (Figure **1d**).

Fig. 1. FT-IR spectra of (**a**) graphite, (**b**) GO, (**c**)GO-HPG, and (**d**) GO-HPG-IA.

Figure **2** depicts XRD patterns of graphite and GO, respectively. The XRD pattern of graphite exhibits a peak at approximately 2θ= 26.5º, corresponding to the interlayer distance of 0.335nm (Figure 2a). In Figure **2b**, the peak at 2θ = 12.7° represented graphene oxide. The interlayer spacing (d-spacing) of GO was calculated 0.78 nm which indicated the formation of oxygen-containing functional groups between the layers of the graphite.

Fig. 2. XRD patterns of (**a**) graphite, (**b**) GO

In Figure 3 the TGA thermograms of (a) GO, (b) GO-HPG and (c) GO-HPG-IA are displayed. As seen from Figure 3a, the first weight loss below 110 ºC can be assigned to trapped water between GO nanosheets. Also, there is a major weight loss between 110 °C and 360 °C due to the decomposition of the labile oxygen-containing functional groups on the GO, and the third step above 400°C assigned to an unstable carbon remaining [39]. As shown in Figure **3b** and **c**, the GO-HPG and GO-HPG-IA are more stable than GO, which demonstrates

the HPG has been successfully grafted on to the GO surface. For the GO-HPG curve, the weight loss below 100 ºC is assigned to removal of physically adsorbed water. The second weight loss about 33% occur at the temperatures ranging from 260 ºC to 370 ºC, and it is attributed to the chemical grafting of HPG on to the GO surface (Figure **3b**) [40]. After reacting with isatoic anhydride, the weight loss of the curve in Figure **3c** between 290–400 ºC increase to 39%, confirmed that covalently functionalized GO-HPG.

Fig. 3. TGA graph of (**a**) GO, (**b**) GO-HPG and (**c**) GO-HPG-IA.

Figures **4a** and **4b** exhibit the FE-SEM images of GO and GO-HPG-IA-Cu(II) nanosheets respectively. In Figure **4a**, the observed well-ordered two-dimensional and flake-like sheets of the GO nanosheets. Different morphologies were shown for GO and prepared catalyst. Wrinkled and folded structures of GO-HPG-IA-Cu(II) nanosheets appears that polymers covered the surfaces of graphene oxide (Figure **4b**)[41-42].

Fig. 4. FE- SEM images of (**a**) GO and (**b**) GO-HPG-IA-Cu(II).

Figure **5** shows typical AFM images and the height profiles of GO and GO-HPG-IA-Cu(II) which are occupied to measure their thickness and observe the morphology of GO nanosheets. The AFM images of the GO and GO-HPG-IA-Cu(II) confirm corrugated nature of the grapheme oxide nanosheets. The height profile shows that the average thickness of the GO is about 1nm which proposed a single layer structure (Figure **5a**). The thickness of GO-HPG-IA-Cu(II) is shown in Figure **5b**. In the microscope image of GO-HPG-IA-Cu(II) could

be observed nanosheets with thickness of about 15 nm. The surface uniform coverage illustrates that the polymer chains were nearly equally distributed over the entire surface.

The EDS analysis of GO and GO-HPG-IA-Cu(II) catalyst confirmed the presence of C, O, N, and Cu atoms (Figure **6a**, **b**). Also, the catalyst was evaluated by an inductively coupled plasma (ICP) analyzer. ICP analysis indicated the presence of copper in the catalyst and the content of Cu was measured to be 1.0 mmol g^{-1} (6.4%).

Fig. 5. AFM images of (**a**) GO nanosheets and (**b**) GO-HPG-IA-Cu(II).

Fig. 6. EDS patterns of (**a**) GO and (**b**) GO-HPG-IA-Cu(II).

Investigation of catalyst activity of GO-HPG-IA-Cu(II) in the synthesis of naphthoquinone derivatives

The prepared GO-HPG-IA-Cu(II) was used as heterogeneous catalyst in the synthesis of naphthoquinones. Initially, the reaction parameters were optimized in the one-pot three-component reaction of 2-hydroxy-1,4-naphthoquinone, 4-chlorobenzaldehyde, 4-methoxyanilineas a model reaction underultrasound conditions.

To observe the optimal solvents, the reaction was tested in various solvents such as H_2O,EtOH, acetonitrile, n-hexane, and chloroform (Table **1**, entries 1–5). As shown in Table **1**, entry 5, the yield of reaction in the EtOH is more than other solvents. Moreover, the reactions were clean in EtOH compared to those in organic solvents. Therefore, EtOH were chosen as the reaction medium. In order to obtain the optimal amount of the catalyst, the reaction was carried out in the presence of different amounts of catalyst. The best result was

observed with 15 mg of the catalyst (0.1 mol% Cu) and the productyield afforded 94% at 5 min in EtOH under ultrasound conditions (Table **1**, entry 5). Also, the reaction was performed in the absence of catalyst and no product was formed (Table **1**, entry 6). As shown in Table **1**, we observed effecting of ultrasonic irradiation frequency (rang of 20-45 kHz) on reaction. When the reaction was performed in the absence of ultrasonic irradiation, the product was not obtained at room temperature for 60 min (Table **1**, entry 10), while in the presence of ultrasonic irradiation at power of 40 kHz and GO-HPG-IA-Cu(II) catalyst, the yield increased to 94% after 5 min (Table **1**, entry 5).

Therefore, the best result was achieved with 15 mg (0.1mol% Cu) of GO-HPG-IA-Cu(II) as catalyst in EtOH under ultrasonic irradiation with power of 40 kHz afforded 2-((4-chlorophenyl)((4-methoxyphenyl)amino)methyl)-3-hydroxynaphthalene-1,4-dione at 5 min with 94 % yield.

Table 1. Optimizing the reaction conditions [a]

After optimization of the reaction conditions, synthesis of naphthoquinone derivatives were carried out for a series of different aromatic aldehydes containing electron-releasing and electron-withdrawing substituents to investigate the versatility of the protocol under GO-HPG-IA-Cu(II) catalysis. As shown in Table **2**, aromatic aldehydes containing electron-withdrawing groups reacted rapidly and gave higher yields, while substitutions of electron-rich groups on the benzene ring required longer reaction times and got lower yields. It seems that the electron-donating groups decrease the electrophilicity of the carbonyl group, leading to longer reaction times and little lower yields. Furthermore, the structures of these products were supported by ^{1}H NMR spectra.

Table 2. Synthesis of naphthoquinone derivatives catalyzed by GO-HPG-IA-Cu(II) [a].

As shown in Figure **7**, we examined the reusability of GO-HPG-IA-Cu(II) as heterogeneous catalyst for the same reactants. After completion of the reaction, the catalyst was isolated by filtration, washed exhaustively with chloroform, and ethanol and drying at 80 °C in an oven for 24h for subsequent experiments to check its reusability under similar reaction conditions. The recycled catalyst could be reused for five times without considerable loss of its catalytic activity and gave the corresponding product in high yields. Afterwards, the product melting point was checked to ensure that the purity remained excellent.

Fig. 7. The reusability of the catalyst GO-HPG-IA-Cu(II) in the synthesis of naphthoquinone derivatives.

The proposed reaction mechanism

A possible mechanism for the synthesis of naphthoquinone derivatives is depicted in Scheme **2**. Firstly, the aldehyde is activated by the GO-HPG-IA-Cu(II) catalyst to give (I) which upon nucleophilic attack of amine to form imine (II). Subsequently, 2-hydroxynaphthalene-1,4-dione attacks imine (II) in the presence of the GO-HPG-IA-Cu(II) catalyst to provide intermediate (III), which undergoes tautomeric proton shift to generate the naphthoquinone derivatives and releases the catalyst for the next run.

Scheme 2. Proposed mechanism for synthesis of naphthoquinone derivatives.

Conclusion

In conclusion, we have successfully introduced a clean, eco-friendly, efficient and cost-effective synthesis of naphthoquinones under ultrasound irradiation. Furthermore, we have designed a heterogeneous catalyst based on Go-HPG-IA-Cu(II). In this research, a facile strategy for grafting of PG onto the surface of GO nanosheets is demonstrated. This PG layer on graphene oxide surface not only stabilize Cu(II) intermediates but also advance the catalytic process. The catalyst was easily recovered and reused five cycles without a significant loss of catalytic activity and given products with high yields in short time.

Acknowledgements

The authors are grateful to University of Kashan for supporting this work by Grant No. 159148/86.

References

1. Hunger, K. *Industrial dyes: chemistry, properties, applications*. John Wiley & Sons2007.

2. Aldakov, D.; Anzenbacher Jr, P., *ChemComm* **2003,** (12), 1394.

3. Belgodere, E.; Bossio, R.; Chimichi, S.; Parrini, V.; Pepino, R., *Dyes Pigm* **1983,** *4* (1), 59. doi: 10.1016/0143-7208(83)80007-2.

4. Dabiri, M.; Tisseh, Z. N.; Bazgir, A., *Dyes Pigm* **2011,** *89* (1), 63. doi: 10.1016/j.dyepig.2010.09.004.

5. Shaabani, S.; Naimi-Jamal, M. R.; Maleki, A., *Dyes Pigm* **2015,** *122*, 46. doi: 10.1016/j.dyepig.2015.06.013.

6. Allochio Filho, J. F.; Fiorot, R. G.; Lacerda, V.; dos Santos, R. B.; Vanini, G.; Romão, W.; Greco, S. J., *Colloid Interface Sci. Commun.* **2015,** *4*, 14. doi: 10.1016/j.colcom.2015.03.002.

7. Shaterian, H. R.; Mohammadnia, M., *J. Mol. Liq.* **2013,** *177*, 353. doi: 10.1016/j.molliq.2012.10.012.

8. Fiorot, R. G.; Allochio Filho, J. F.; Pereira, T. M.; Lacerda, V.; dos Santos, R. B.; Romão, W.; Greco, S. J., *Tetrahedron Lett.* **2014,** *55* (31), 4373. doi: 10.1016/j.tetlet.2014.06.031.

9. Tavakoli, H. R.; Moosavi, S. M.; Bazgir, A., *Res. Chem. Intermed.* **2015,** *41* (5), 3041. doi: 10.1007/s11164-013-1413-8.

10. Shaterian, H. R.; Moradi, F., *Res. Chem. Intermed.* **2015,** *41* (1), 291. doi: 10.1007/s11164-013-1191-3.

11. Bolotin, K. I.; Sikes, K.; Jiang, Z.; Klima, M.; Fudenberg, G.; Hone, J.; Kim, P.; Stormer, H., *Solid State Communications* **2008,** *146* (9), 351. doi: 10.1016/j.ssc.2008.02.024.

12. Morozov, S.; Novoselov, K.; Katsnelson, M.; Schedin, F.; Elias, D.; Jaszczak, J. A.; Geim, A., *Phys. Rev. Lett.* **2008,** *100* (1), 016602. doi: 10.1103/PhysRevLett.100.016602.

13. Lee, C.; Wei, X.; Kysar, J. W.; Hone, J., *Science* **2008,** *321* (5887), 385. doi: 10.1126/science.1157996.

14. Balandin, A. A.; Ghosh, S.; Bao, W.; Calizo, I.; Teweldebrhan, D.; Miao, F.; Lau, C. N., *Nano Lett.* **2008,** *8* (3), 902. doi: 10.1021/nl0731872.

15. Cai, W.; Zhu, Y.; Li, X.; Piner, R. D.; Ruoff, R. S., *Appl. Phys. Lett.* **2009,** *95* (12), 123115. doi: 10.1063/1.3220807.

16. Li, X.; Zhu, Y.; Cai, W.; Borysiak, M.; Han, B.; Chen, D.; Piner, R. D.; Colombo, L.; Ruoff, R. S., *Nano Lett.* **2009,** *9* (12), 4359. doi: 10.1021/nl902623y.

17. Ruoff, R., *Nat. Nanotechnol.* **2008,** *3* (1), 10. doi: 10.1038/nnano.2007.432.

18. Eda, G.; Chhowalla, M., *Adv. Mater* **2010,** *22* (22), 2392. doi: 10.1002/adma.200903689.

19. Li, X.; Zhang, G.; Bai, X.; Sun, X.; Wang, X.; Wang, E.; Dai, H., *Nat. Nanotechnol.* **2008,** *3* (9), 538. doi: 10.1038/nnano.2008.210.

20. Kim, F.; Cote, L. J.; Huang, J., *Adv. Mater* **2010,** *22* (17), 1954. doi: 10.1002/adma.200903932

21. Su, C.; Loh, K. P., *Acc. Chem. Res.* **2012,** *46* (10), 2275. doi: 10.1021/ar300118v.

22. Gao, C.; Yan, D., *Progress in Polymer Science* **2004,** *29* (3), 183. doi: 10.1016/j.progpolymsci.2003.12.002.

23. Zarrabi, A.; Adeli, M.; Vossoughi, M.; Shokrgozar, M. A., *Macromol. Biosci.* **2011,** *11* (3), 383. doi: 10.1002/mabi.201000336

24. Adeli, M.; Haag, R.; Zarnegar, Z., *J. Nanopart. Res.* **2007,** *9* (6), 1057. doi: 10.1007/s11051-006-9188-0.

25. Roller, S.; Türk, H.; Stumbé, J.-F.; Rapp, W.; Haag, R., *J. Comb. Chem.* **2006,** *8* (3), 350. doi: 10.1021/cc050139b.

26. Haag, R.; Stumbé, J.-F.; Sunder, A.; Frey, H.; Hebel, A., *Macromolecules* **2000,** *33* (22), 8158. doi: 10.1021/ma000831p.

27. Istratov, V.; Kautz, H.; Kim, Y.-K.; Schubert, R.; Frey, H., *Tetrahedron* **2003,** *59* (22), 4017. doi: 10.1016/S0040-4020(03)00470-8.

28. Schüll, C.; Frey, H., *Polymer* **2013,** *54* (21), 5443. doi: 10.1016/j.polymer.2013.07.065.

29. Anastas, P. T.; Warner, J. C. *Green chemistry: theory and practice*. Oxford university press2000.

30. Cravotto, G.; Cintas, P., *Chem. Soc. Rev.* **2006,** *35* (2), 180. doi: 10.1039/B503848K.

31. Suslick, K. S.; Nyborg, W. L., *The Journal of the Acoustical Society of America* **1990,** *87* (2), 919. doi: 10.1121/1.398864.

32. Zang, H.; Su, Q.; Mo, Y.; Cheng, B.-W.; Jun, S., *Ultrason. Sonochem.* **2010,** *17* (5), 749. doi: 10.1016/j.ultsonch.2010.01.015.

33. Dabiri, M.; Tisseh, Z. N.; Bahramnejad, M.; Bazgir, A., *Ultrason. Sonochem.* **2011,** *18* (5), 1153. doi: 10.1016/j.ultsonch.2010.12.004.

34. Naeimi, H.; Shaabani, R., *Ultrason. Sonochem.* **2017,** *34*, 246. doi: 10.1016/j.ultsonch.2016.05.043.

35. Li, J.-T.; Sun, M.-X.; Yin, Y., *Ultrason. Sonochem.* **2010,** *17* (2), 359. doi: 10.1016/j.ultsonch.2009.09.004.

36. Cai, N.; Li, C.; Luo, X.; Xue, Y.; Shen, L.; Yu, F., *J. Mater. Sci.* **2016,** *51* (2), 797. doi: 10.1007/s10853-015-9403-4.

37. Stankovich, S.; Dikin, D. A.; Piner, R. D.; Kohlhaas, K. A.; Kleinhammes, A.; Jia, Y.; Wu, Y.; Nguyen, S. T.; Ruoff, R. S., *carbon* **2007,** *45* (7), 1558. doi: 10.1016/j.carbon.2007.02.034.

38. Pham, T. A.; Kumar, N. A.; Jeong, Y. T., *Synth. Met* **2010,** *160* (17), 2028. doi: 10.1016/j.synthmet.2010.07.034.

39. Gkikas, M.; Theodosopoulos, G. V.; Das, B. P.; Tsianou, M.; Iatrou, H.; Sakellariou, G., *Eur. Polym. J.* **2014,** *60*, 106. doi: 10.1016/j.eurpolymj.2014.08.022.

40. Lee, S. H.; Dreyer, D. R.; An, J.; Velamakanni, A.; Piner, R. D.; Park, S.; Zhu, Y.; Kim, S. O.; Bielawski, C. W.; Ruoff, R. S., *Macromol. Rapid Commun.* **2010,** *31* (3), 281. doi: 10.1002/marc.200900641.

41. Landarani-Isfahani, A.; Taheri-Kafrani, A.; Amini, M.; Mirkhani, V.; Moghadam, M.; Soozanipour, A.; Razmjou, A., *Langmuir* **2015,** *31* (33), 9219. doi: 10.1021/acs.langmuir.5b02004.

42. Asadi, B.; Mohammadpoor-Baltork, I.; Tangestaninejad, S.; Moghadam, M.; Mirkhani, V.; Landarani-Isfahani, A., *New J. Chem* **2016,** *40* (7), 6171. doi: 10.1039/C5NJ03050A.

1.

Fig. 1. FT-IR spectra of (**a**) graphite, (**b**) GO, (**c**)GO-HPG, and (**d**) GO-HPG-IA.

Fig. 2. XRD patterns of (**a**) graphite, (**b**) GO

Fig. 3. TGA graph of (**a**) GO, (**b**) GO-HPG and (**c**) GO-HPG-IA.

Fig. 4. FE- SEM images of (**a**) GO and (**b**) GO-HPG-IA-Cu(II).

Fig. 5. AFM images of (**a**) GO nanosheets and (**b**) GO-HPG-IA-Cu(II).

Fig. 6. EDS patterns of (**a**) GO and (**b**) GO-HPG-IA-Cu(II).

Table 1. Optimizing the reaction conditions [a]

Fig. 7. The reusability of the catalyst GO-HPG-IA-Cu(II) in the synthesis of naphthoquinone derivatives.

Scheme 1. Preparation of GO-HPG-IA-Cu(II) nanocatalyst.

Scheme 2. Proposed mechanism for synthesis of naphthoquinone derivatives.

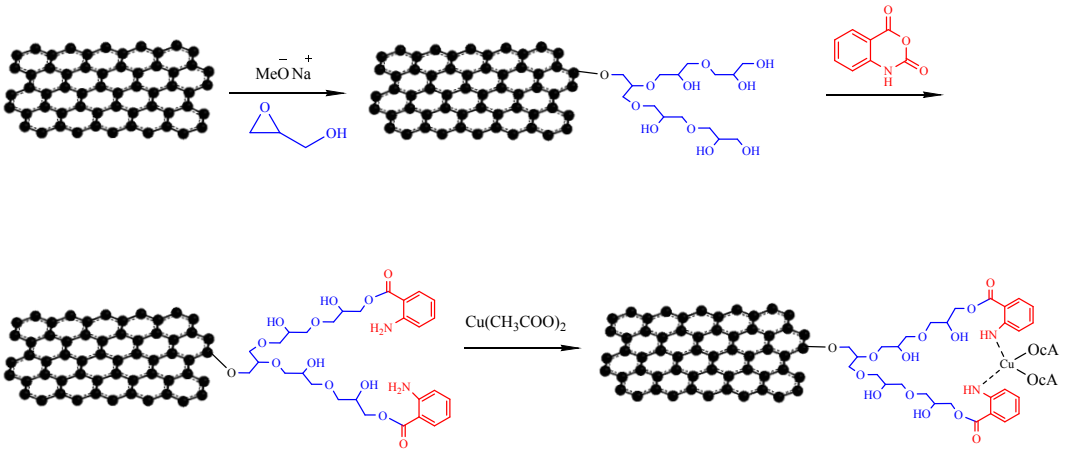

Scheme 1. Preparation of GO-HPG-IA-Cu(II) nanocatalyst.

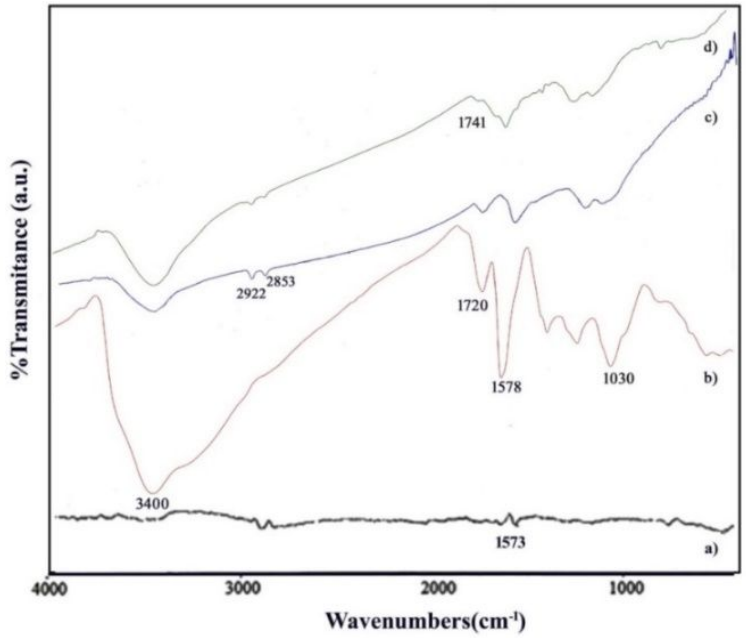

Fig. 1. FT-IR spectra of (**a**) graphite, (**b**) GO, (**c**)GO-HPG, and (**d**) GO-HPG-IA.

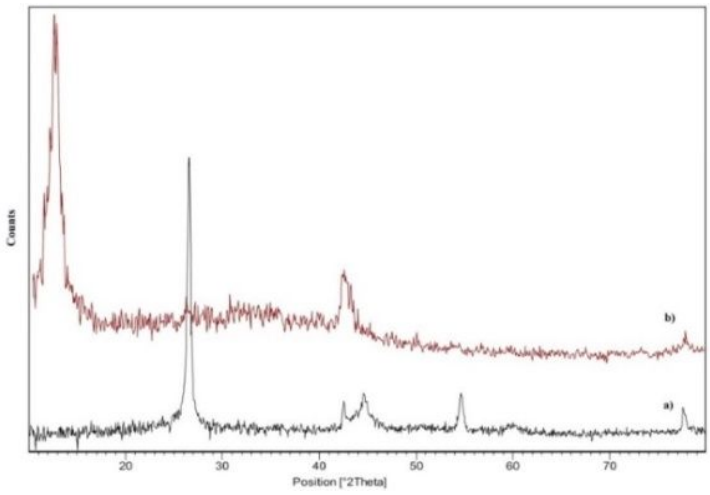

Fig. 2. XRD patterns of (**a**) graphite, (**b**) GO

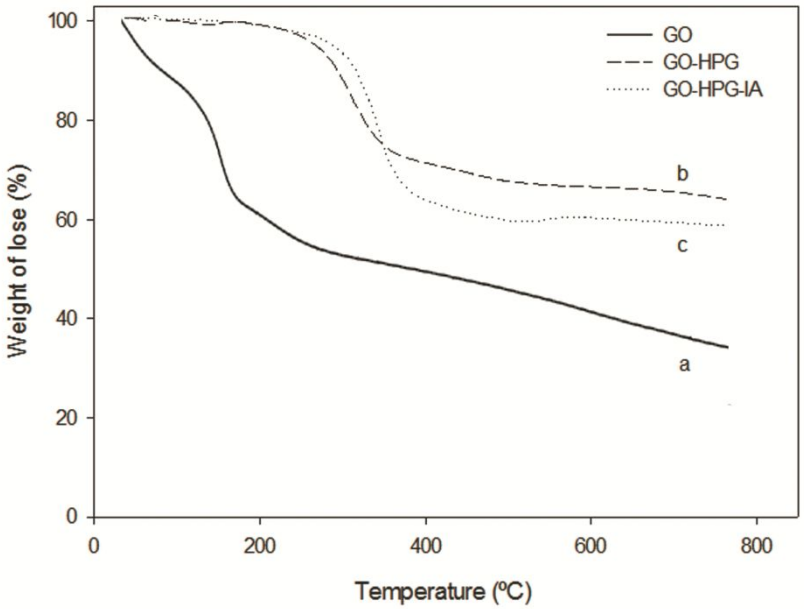

Fig. 3. TGA graph of (**a**) GO, (**b**) GO-HPG and (**c**) GO-HPG-IA.

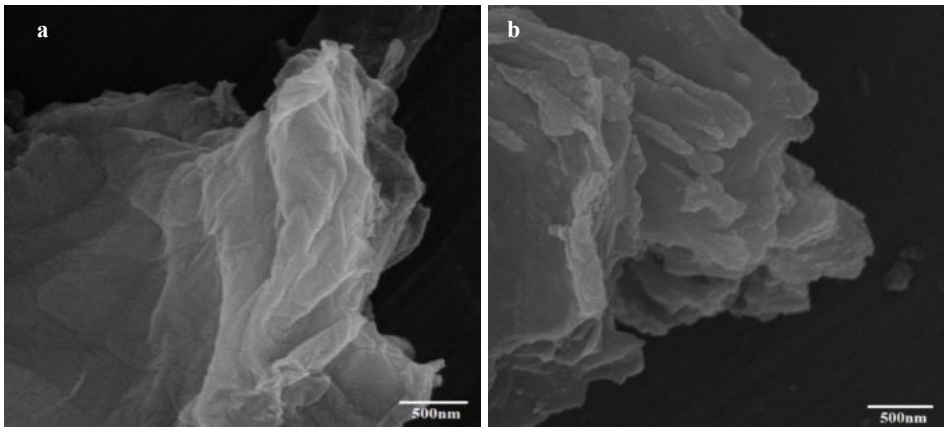

Fig. 4. FE- SEM images of (**a**) GO and (**b**) GO-HPG-IA-Cu(II).

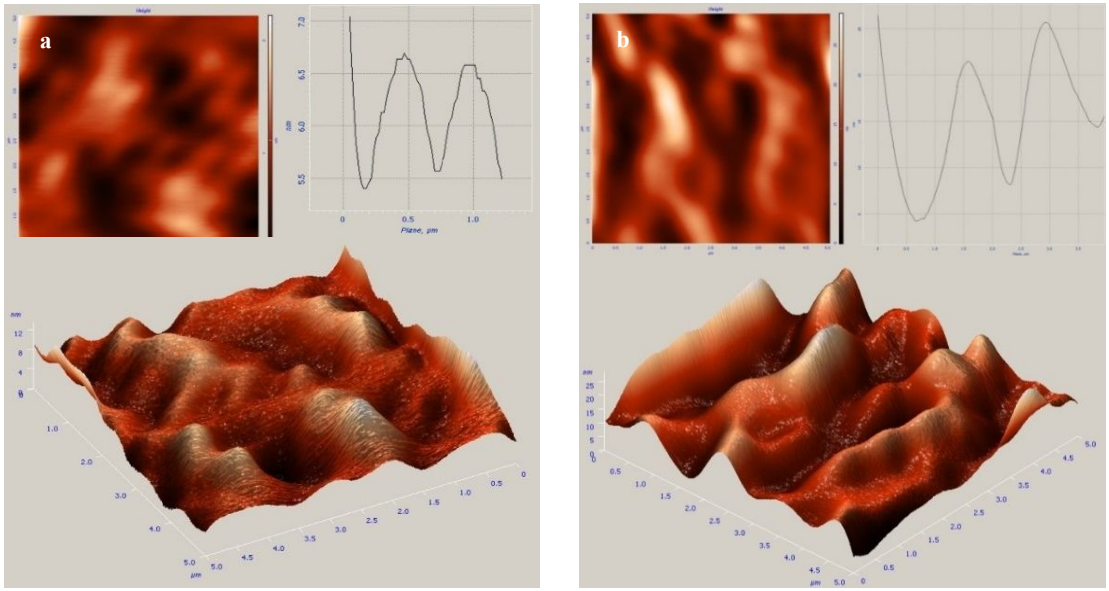

Fig. 5. AFM images of (**a**) GO nanosheets and (**b**) GO-HPG-IA-Cu(II).

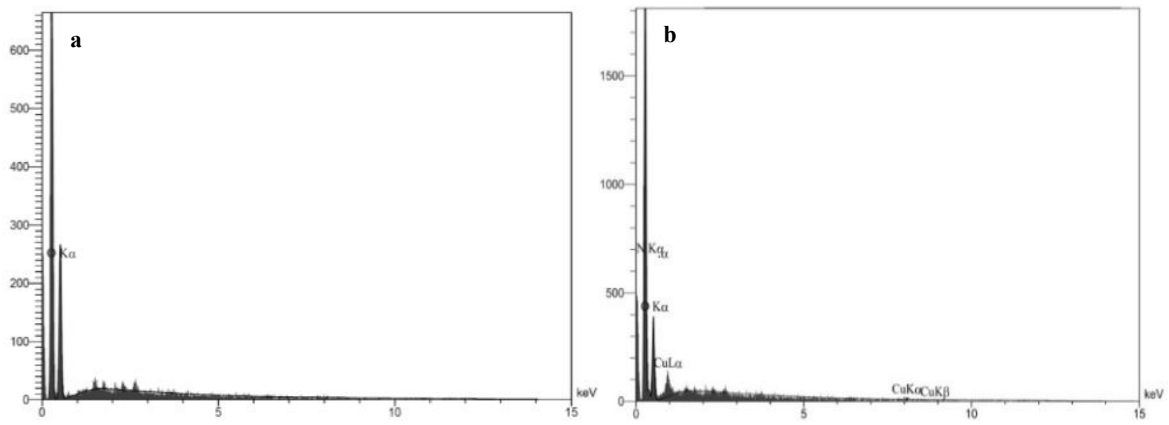

Fig. 6. EDS patterns of (**a**) GO and (**b**) GO-HPG-IA-Cu(II).

Table 1. Optimizing the reaction conditions [a]

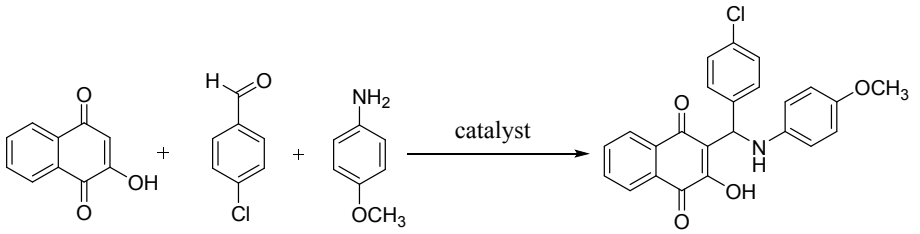

Entry	Solvent	US.F (kHz)	Catalyst (mg)	Time (min)	Yield[b] (%)
1	H_2O	40	15	10	Trace
2	CH_3CN	40	15	10	70
3	n-hexane	40	15	20	35
4	$CHCl_3$	40	15	20	40
5	EtOH	40	15	5	94
6	EtOH	40	0	15	-
7	EtOH	40	5	10	78
8	EtOH	40	10	10	81
9	EtOH	40	20	5	94
10	EtOH	-	15	60	-
11	EtOH	20	15	10	55
12	EtOH	35	15	10	80
13	EtOH	45	15	5	94

[a] Reaction conditions: 2-hydroxy-1,4-naphthoquinone (1 mmol), aldehyde (1 mmol), amine(1 mmol)), GO-HPG-IA-Cu(II). [b] Isolated yields.

Table 2. Synthesis of naphthoquinone derivatives catalyzed by GO-HPG-IA-Cu(II) [a].

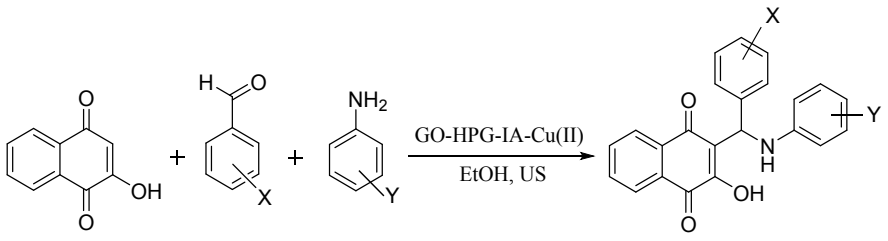

1 **2** **3** **4a-m**

T (min), Yield[b](%), TON, TOF (h^{-1})			
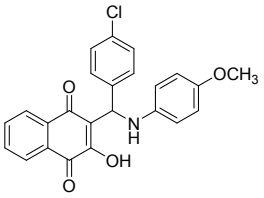	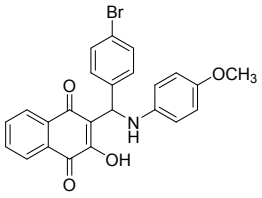	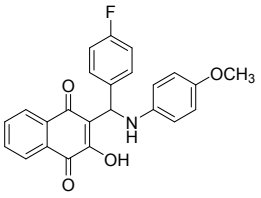	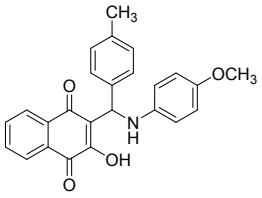
5, 94, 63, 755	5, 94, 63, 755	10, 90, 60, 353	10, 84, 56, 329
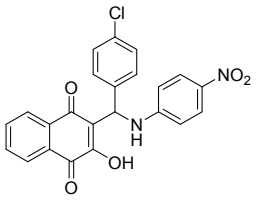	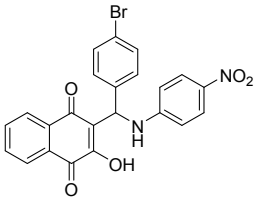	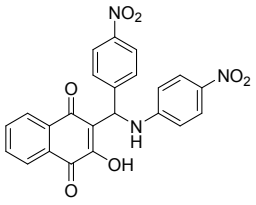	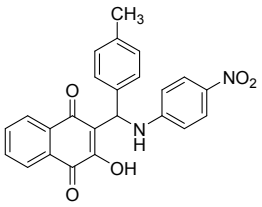
15, 85, 57, 227	15, 85, 57, 227	10, 93, 62, 365	15, 80, 53, 213
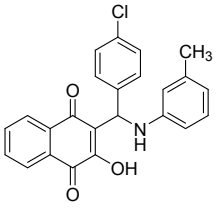	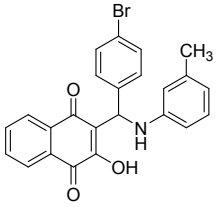	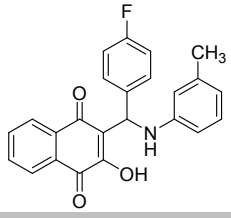	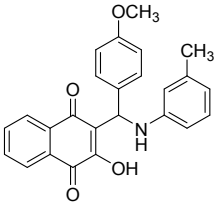
10, 94, 63, 369	10, 94, 63, 369	15, 84, 56, 224	15, 80, 53, 213
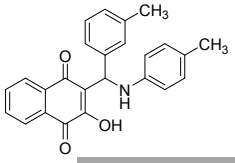			
10, 82, 55, 322			

[a] Reaction conditions: 2-hydroxy-1,4-naphthoquinone (1 mmol), aldehyde (1 mmol), amine (1 mmol), GO-HPG-IA-Cu(II) (15 mg, 0.1 mol%), EtOH, under ultrasound conditions. b Isolated yields. c TON: mole of formed naphthoquinone derivatives per mole of catalyst. d TOF (h^{-1}): (mmol of product/mmol of active site of catalyst)/time of the reaction (h).

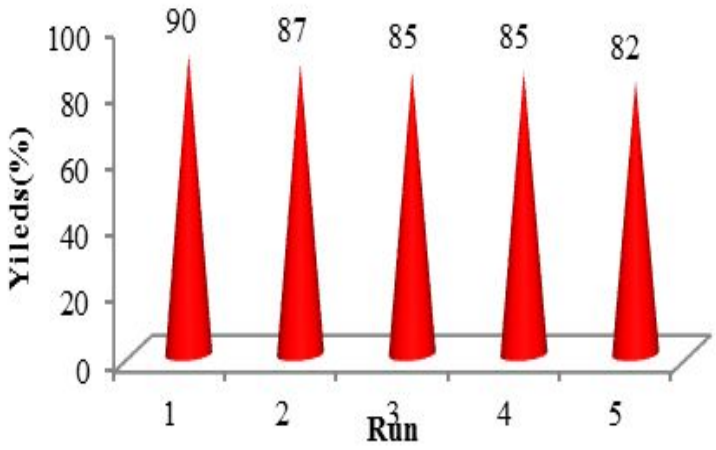

Fig. 7. The reusability of the catalyst GO-HPG-IA-Cu(II) in the synthesis of naphthoquinone derivatives.

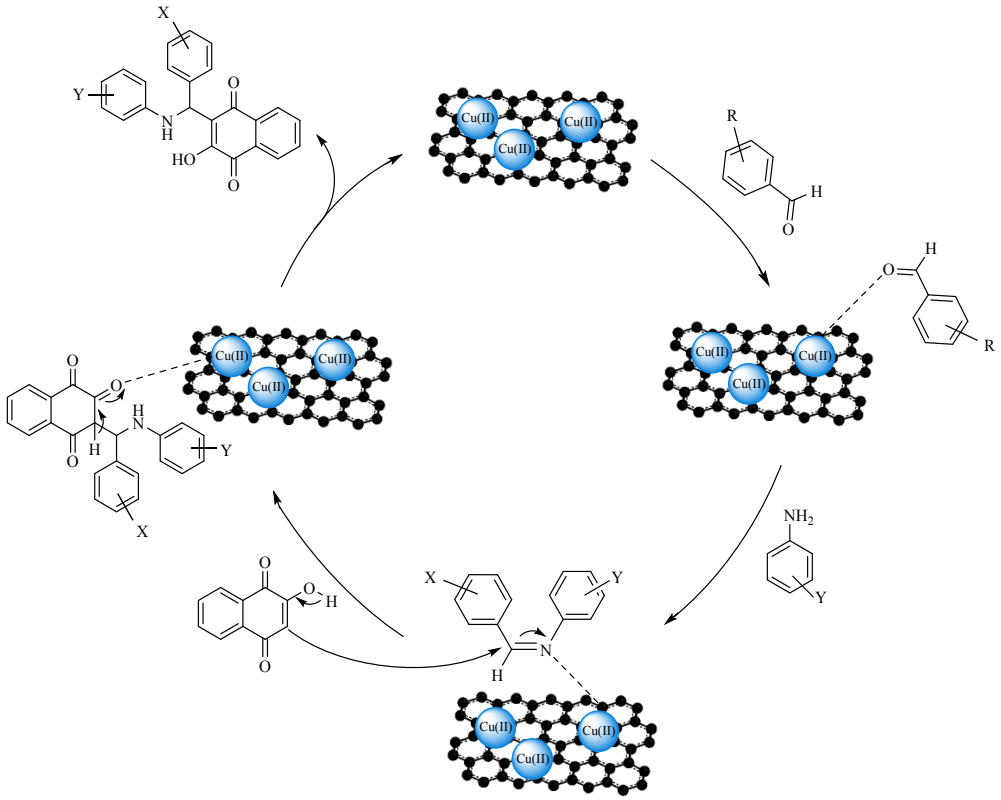

Scheme 2. Proposed mechanism for synthesis of naphthoquinone derivatives.